smaller. Therefore, the dose to the OARs will be wrongly estimated if the MIP scan is used for delineation.

PO-0845

Evaluation of interplay effects of target and MLC during VMAT by using 3D gel measurements

S. Ceberg[1], C. Ceberg[2], M. Falk[3], P. Munck af Rosenschöld[3], S. Bäck[1]
[1]*Skåne University Hospital, Medical Radiation Physics, Lund, Sweden*
[2]*Lund University, Medical Radiation Physics Department of Clinical Sciences Lund, Lund, Sweden*
[3]*Radiation Medicine Research Center, Radiation Oncology Rigshospitalet, Copenhagen, Denmark*

Purpose/Objective: Two types of dosimetric effects due to intra-fractional organ motion has been defined; A) the dose-'blurring' or 'smearing' effect, where the dose delivered to a point in the patient is smeared by the motion of this point in the radiation beam, and B) the interplay effect, where the relative motion between the dynamic MLC leaves and the treatment region may lead to a more complicated dosimetric effect. The aim of this study was to investigate any potential breathing interplay effects during VMAT using 3D polymer gel measurements and compare this with the measurement uncertainty.
Materials and Methods: To simulate tumour movement caused by respiratory motion, the gel phantoms were positioned on a programmable motion platform (Standard Imaging, Inc), which was set to carry out sinusoidal motion. Two different VMAT (RapidArc®, Varian Medical Systems) plans were delivered; a 6 MV small target plan and a 18MV larger target plan. Each delivery was carried out both to a stationary polymer gel phantom and to a gel phantom during motion with a peak-to-peak distance of 20 mm during a period of 4 s and 5 s, respectively. In order to evaluate the dosimetric impact of the interplay between the phantom motion and the dynamic treatment delivery, we defined the dosimetric interplay effect as the relative 3D absorbed dose difference between the volumes obtained from the VMAT measurement during phantom motion and the VMAT measurement to a stationary phantom convolved with the motion function of the moving platform.
Results: The total dosimetric effect of motion was evaluated, i.e. the dose difference between the volume obtained from the measurement during phantom motion and the measurement to a stationary phantom. The isodose volume ≥ 90% was investigated. The mean value and standard deviation of the differences obtained from the measurements were (-3.7±2.6)% for the small target plan and (-4.3±4.8)% for the larger target plan. Investigating the interplay effect, the relative dose difference between the measured VMAT delivery during phantom motion and the convolved stationary VMAT delivery resulted in (-1.2± 1.4)% and (0.9±2.3)% for the small and larger plan, respectively. The results were compared to the dose difference between two repeated stationary convolved gel measurement, which resulted in (0.06±0.5)% and (0.4±0.9)% for the small and larger plan respectively. Although the interplay effects were small compared to the smearing effect, the standard deviations were significantly ($p<0.001$) larger than the narrow distribution for repeated stationary measurement.
Conclusions: The total dosimetric effect due to target motion and dynamic MLC motion during VMAT delivery resulted in an average of about 4% target dose reduction. Comparing with the convolved stationary measurement, which includes only the smoothing effect, the average difference was decreased to around 1%, and the remaining deviation was attributed to interplay effects.

POSTER: PHYSICS TRACK: MANAGEMENT OF INTERFRACTION CHANGES

PO-0846

MR-based adaptive radiotherapy for cervical cancer: A concept of fast, automated IMRT planning

M. Stock[1], G.H. Bol[2], E.M. Kerkhof[2], I.M. Jürgenliemk-Schulz[2], D. Georg[1], J.J.W. Lagendijk[2], B.W. Raaymakers[2]
[1]*Medical University Vienna, Radiation Oncology, Vienna, Austria*
[2]*University Medical Center Utrecht, Radiotherapy, Utrecht, The Netherlands*

Purpose/Objective: Repeated MR imaging during radiotherapy enables treatment adaptation based on soft tissue information. Sufficient contrast permits identification of the target and normal tissues and makes a plan adaptation for cervical cancer irradiation possible. In that context one limiting factor will be time-consuming manual plan generation. The aim is therefore to establish fast automated IMRT planning based on a class solution for offline (dedicated MR outside of the treatment room) or even online (MR-Linac) adaptation.
Materials and Methods: For 10 cervical cancer patients 1 initial CT and MR as well as 4 weekly MRs were available. On those 50 T2-weighted transversal MR scans OAR (bladder, rectum and small bowel) as well as target structures (primary, nodal CTV) were manually contoured by an experienced radiation oncologist. Assuming a plan adaptation concept PTVs with 4mm uniform margin were created. The weekly MRs with their respective structure sets were rigidly registered to the CT based on bony anatomy. Treatment plans were generated using 7 beams (6MV) equally distributed around the patient. For each angle beamlets were calculated for a projected area, which contained the PTVs plus a margin of 4mm. The dose calculation was performed with a GPU-based Monte Carlo code (GPUMCD) using the CT data. GPUMCD enables dose calculation in the absence (0T) and presence of a magnetic field (1.5T). The beamlet weights were determined by the fast inverse dose optimization (FIDO) using a class solution for the constraints of target (prescription dose of45Gy) and OAR structures. Dose constraints for the OAR were chosen to be very demanding and are beyond most criteria mentioned in current clinical studies (e.g. RTOG 0418 or INTERTECC study). Target coverage, OAR sparing and timing issues were analyzed.
Results: 100 plans (1 initial and 4 weekly plans for 10 patients with and without a magnetic field) were generated and all fulfilled the ICRU criterion for targets, e.g. D95>42.75Gy. The dose distributions in the targets were very homogeneous with a mean D1cc of 48.2Gy. Only 5 plans had a D40>40Gy for the bladder (see Fig. 1 - also for rectum and bowel values). For the rectum 30% of the plans had a D50>30Gy. This was mainly the case when the rectum was empty and closely attached to the primary target. In general the D50 for the rectum was not above 35Gy. For the small bowel 4 plans show a D50 above 30Gy. No significant difference between 0T and 1.5T plans could be identified. Assuming the use of one GPU per beam anautomated plan generation within 2 or 5 minutes (0 or 1.5T) could be shown.

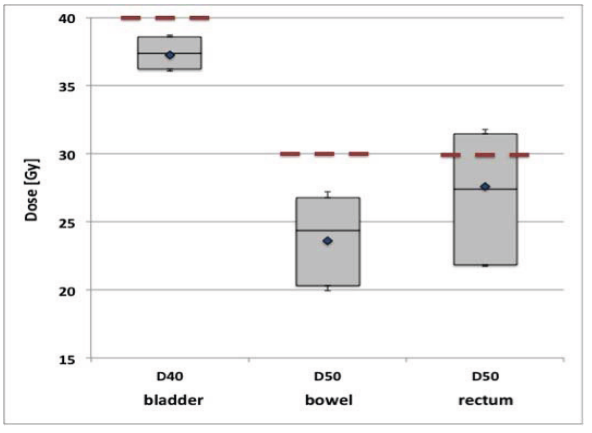

Figure 1: This figure shows the box plot of dose parameters for the respective OAR for the 100 automatically generated plans. Dose planning constraints of the OAR are indicated with a dashed line.

Conclusions: With the current setting automated plans were generated which mostly fulfilled planning criterion. In few cases with insufficient OAR sparing small adaptions of the weight factors for the planning constraints led to acceptable plans. Fast, automated plan generation for cervical cancer using a class solution is possible. Further research will focus on fast, automated contour propagation.

PO-0847

A strategy for non-MU preserving adaptive radiotherapy

W. Crijns[1], H. Van Herck[2], P. Slagmolen[3], K. Haustermans[1], F. Maes[2], F. Van den Heuvel[1]
[1]*University Hospital Gasthuisberg - Radiation Oncology, Laboratory of Experimental Radiotherapy, Leuven, Belgium*
[2]*KULeuven, Departement ESAT/PSI-Medical Image Computing Medical Imaging Research Center, Leuven, Belgium*
[3]*KULeuven, iMinds-KULeuven Future Health Department Leuven Belgium, Leuven, Belgium*

Purpose/Objective: To develop a marker based adaptation strategy, the fluence adaptation of Mohan et al.[1], is combined with a non-MU preserving step taking into account tumor depth and heterogeneities.
Materials and Methods: The adaptation has a geometric and a dosimetric step. The geometric step contains:
· A rigid jaw translation using the average detected marker displacement in the BEV. The field sizes and consequently the MU are preserved.

· A thin plate spline deformation, adapting the original fluence$_0$ into fluence$_X$. In contrast to Ref.[1] marker positions are used instead of organ contours.
· An adapted leaf motion, calculated in Eclipse (Varian Medical Systems, Palo Alto, CA).
For the dosimetric step ray tracing[5] is used to calculate the radiological path length *d*, from the source to each marker. Next, the tissue to phantom ratio, *TPR(0.5,d)*, is calculated using a fixed 0.5cm field size. The TPR_{planX} / TPR_{plan0}-median over the different markers rescales the number of monitor units of each beam.
For validation a 5 beam sliding window IMRT plan is optimized for the TG119 prostate structures[2]. The phantom is extended with 4 markers and bony anatomy. The initial plan$_0$ delivers 77Gy(2.2Gy/Fr). Fractions are simulated by applying translations and isotropic scaling using literature values (Table 1). The isotropic expansion is derived from the shrinkage factor, and is used to evaluate the robustness of our approach.

	Type	Magnitude	Structures
T1	Rigid translation[3] (Lat, Vrt, Lng) [mm]	(-0.4, 2.5, -2.6)	All
T2		(-4.7, 8.2, -8.0)	
T3		(-9.0, 14.9, -13.4)	
S1	Isotropic shrinkage[4]	Expansion factor = 0.9	Target + Markers
E1	Isotropic expansion[4]	Expansion factor = 1.1	

Table 1: Overview of the applied deformations. The type and magnitude are listed in column 2 and 3. Column 4 indicates on which structures the deformations are applied.

Results: Results are compared to plan$_0$ and our clinical standard: shifting of the phantom according to the detected marker positions, see Figure 1.
The combination of the geometric and dosimetric adaptation results in an identical target coverage as was intended (plan$_X$ = plan$_0$). The geometric adaptation alone reduces target coverage compared to plan$_0$ (upper left), similar as our clinical practice (upper row, dashed line (left) vs. solid gray line (right)). All translations have similar results.

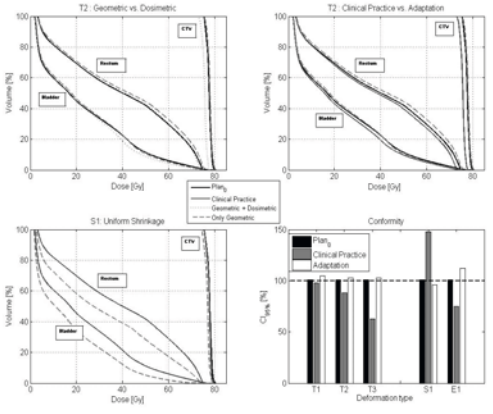

Figure 1. The DVH and conformity results. DVHs of a transformation (T2 upper row), and target shrinkage (S1,E1 lower row) are depicted.

For S1 and E1 a strongly improved conformity is observed for the adaptation compared to the clinical practice (Figure1). The adaptation ensures a stable, better CI_{95} compared to our clinical practice for all applied deformations, this indicates better OAR protection.
Conclusions: Target coverage, conformity, and as consequence OAR protection is improved by the presented non-MU preserving adaptation.
References
1. Mohan, R. *et al. Int. J. Radiat Oncol, Biol, Phys* **61**, (2005).
2. Ezzell, G. a. *et al. Med. Phys.* **36**, (2009).
3. Van den Heuvel, F. *et al. Med. Phys.* **30**, (2003).
4. Budiharto, T. *et al. Radiother Oncol* **90**, (2009).
5. Siddon, R. *Med. Phys.* **12**, (1985).

PO-0848
Image-guided lung stereotactic treatments with the vero system
C. Garibaldi[1], A.M. Ferrari[2], S. Comi[1], A. Surgo[2], G. Piperno[2], F. Pansini[1], M. Cannella[2], A. Rampinelli[2], D. Ciardo[2], R. Orecchia[2]
[1]*European Institute of Oncology, Medical Physics, Milan, Italy*
[2]*European Institute of Oncology, Radiation Oncology, Milan, Italy*

Purpose/Objective: To analyse the accuracy of image-guidance using the cone-beam CT technology of the VERO SBRT system in stereotactic radiotherapy of lung tumors.
Materials and Methods: So far 22 consecutive patients have been treated with stereotactic treatment using the VERO system (BrainLAB AG, Mitsubishi Heavy Industries). A free breathing CT scan and a 10-phase respiration correlated 4D-CT to allow patient-specific motion assessment were acquired with a slice thickness of 2.5 mm. The Real-time Position Management respiratory gating system (RPM, Varian) was used to generate the external breathing signal and to retrospectively correlate cine CT images with the breathing phases. Patients, positioned supine with an arm holder (Posirest, Civco), were trained to achieve a regular breathing with the aid of a wearable display showing the breathing cycle. The internal target volume (ITV) was obtained contouring the tumor on the reconstructed maximum intensity projection and the mean intensity projection CT images. The PTV was generated with a safety margin of 5 mm to account for setup uncertainties. Treatment plans, consisting of 1-3 non coplanar conformal dynamic arcs or multiple IMRT fields, were generated for the VERO system. Doses between 25 and 54 Gy were delivered to the isocenter in 3 to 5 fractions. Patients were setup according to Exactrac and target localization was achieved with a kV-CBCT. Due to the limited field of view, in most of the cases the vertebral spine was not visible for evaluation of the patient set-up. The clipbox for automatic soft-tissue registration of the CBCT and the planning CT was confined around the lesion. The radiation oncologist then performed a manual registration to adjust the position of the ITV and PTV to the motion-blurred tumor in all three planes in the CBCT. Translational and rotational target localization errors were corrected with the 5 degree-of-freedom robotic couch and the ring rotation. A verification CBCT was acquired after correction to evaluate residual errors. If residual error was greater than 2 mm in any direction, a second correction was made and another CBCT acquired.
Results: In the table are shown the group mean, the systematic (Σ) and random (σ) component of the tumor localization errors and residual errors after correction, in terms of translations and rotations. Data were obtained from the analysis of 168 CBCTs. The mean 3D vector at initial set-up was 5.7±1.4 mm, while was significantly reduced to 1.4±0.6 mm after 6D automatic correction.

		Translations (mm)				Rotations (°)		
		LR	SI	AP	3D vector	roll	pitch	yaw
Tumor localization	**Group mean**	**0.5**	**1.7**	**-3.4**	**5.7**	**0.6**	**0.0**	**0.1**
error	**Σ**	**1.2**	**3.2**	**1.9**	**1.4**	**0.7**	**1.0**	**1.0**
	σ	**1.7**	**2.3**	**1.9**	**1.9**	**0.8**	**0.9**	**1.4**
Residual error	**Group mean**	**-0.1**	**0.0**	**0.0**	**1.4**	**-0.1**	**0.0**	**0.0**
	Σ	**0.5**	**0.7**	**0.6**	**0.6**	**0.3**	**0.2**	**0.3**
	σ	**0.5**	**1.0**	**1.0**	**1.0**	**0.4**	**0.4**	**0.3**

Conclusions: On-line CBCT image guidance and automatic 6D correction available on the VERO system allowed a very accurate tumor localization in lung stereotactic treatments. A post-treatment CBCT will be acquired in the next group of patients to assess the safety margins required to compensate for residual positional uncertainties and intra-fraction tumor displacement.

PO-0849
Dose coverage of lymph nodes in treatments corrected for daily baseline shift of the primary tumour
T.B. Nielsen[1], C. Brink[1]
[1]*Laboratory of Radiation Physics, Odense University Hospital, DK-5000 Odense, Denmark*

Purpose/Objective: Treatment planning and irradiation of lung cancer patients are often based on the mid-ventilation phase in order to minimize planning margins. The primary lung tumour and involved lymph node located in the mediastinum region can have different respiratory patterns. There can be a systematic baseline shift across the entire treatment course between the primary tumour and the lymph node as well as daily random baseline variations. It is desirable to correct for baseline shifts that occurs daily for the primary lung tumour but that might cause a discrepancy between the planned and delivered dose distribution to the lymph node. This study investigates the dose coverage of the lymph node when the entire dose distribution is shifted in accordance with baseline shift of the primary tumour.